

Investigation on the Validity Region of Online Combustion and Torque Models of Gasoline Engines with Retarded Ignition

Fangwu Ma and Zheng Qu

Abstract The recently proposed online mean-value thermodynamic combustion model suffers from its error-prone CA50 prediction. In an effort to improve the accuracy of CA50 prediction in the case of ignition retard, this paper demonstrates the convergence of normalized IMEPH-CA50 predictions towards a unanimous characteristic curve indiscriminately for various gasoline engine selections, speeds and loads. For the first time, this paper reveals the physical principle of a characteristic curve via an ideal-heat-release model and thereby formulates a validity region of the IMEPH-CA50 predictions. The predicted values outside of the region will then be corrected by a surrogate of the characteristic curve. In this way, ECUs successfully identify invalid CA50 predictions online and modulate them towards the actual values. Large-scale experiments have shown the developed method improves the accuracy in CA50 prediction, while preserving the high accuracy of IMEPH prediction.

Keywords Torque model · Gasoline engine · Prediction accuracy · Validity region · Ignition retard

F2012-A05-007

F. Ma (✉) · Z. Qu
Geely Automobile Research Institute, Hangzhou, China
e-mail: mafw@rd.geely.com

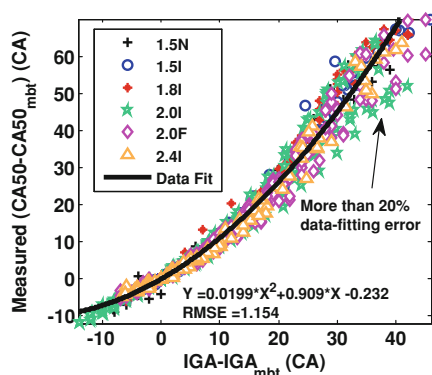
1 Introduction

Recent soaring gasoline price has placed a higher demand on gasoline engine control for the purpose of higher fuel efficiency. To optimize the control of air flow, modern vehicles replace the mechanical throttle with electronic throttle control (ETC.) for complete air path control [1, 2]. As a result, a valid torque model is required in order to project the desired driver torque to the desired air mass [3]. In the case of ignition angle (IGA) retard, the required air amount can vary vastly because torque magnitude can be altered by late ignition [4]. Current engine control units (ECU) makers have developed a simple torque model to represent the late IGA effects. The model uses a parabolic data-fitted curve to map a retarded ignition angle (IGA) to a normalized indicated-mean-effective-pressure-high (IMEPH) loss, which is named as the “data-fitted torque model”. To further cut the cost, ECU makers have been practicing to use a unique model to support all engine fleets on the market. For years, this model has been considered sufficient in fulfilling the requirement of torque prediction accuracy for all gasoline engines. The data proof of this action, however, has been scarce in literature.

This paper demonstrates large IMEPH-IGA dataset over wide range of engine selections and evaluates the model performance with numerical proof. In Sect. 2.1, a normalized graph will render the torque data in the entire operation range and thereby reveal both the performance and limitation of the data-fitted torque model. The major limitation is found to be the large model error in large IGA retard region. In order to renovate the accuracy in the particular region, the authors recently proposed an online mean-value thermodynamic combustion model that generates cycle-to-cycle IMEPH and CA50 prediction [5, 6]. When applied to the case of ignition retard, the new model has shown more accuracy and robustness in torque prediction compared with that of a data-fitted model. This paper will further expound the amount of improvement in IMEPH precision with large-scale data proof. Meanwhile, this paper will also investigate into the quality of model’s CA50 prediction and develop a method to explore its use in torque validity diagnosis.

With fluid energy dynamics fully monitored, the online combustion model can provide real-time prediction of combustion phasing, such as 50 % fuel burn moment (CA50). This feature turns out to be equally important as the torque prediction capability in today’s engine control design, because CA50 has been widely used as the most representative index of combustion quality [7–9]. Some advanced control strategy relies heavily on the knowledge of CA50. One example is the self-calibration scheme that modulates the VVT set-points according to the real-time knowledge of torque and CA50 [8], in which way an engine can defy aging and maintain high efficiency throughout its life. There has been an effort to incorporate the online combustion model with the self-calibration scheme. No significant success has been made due to more than 15 % averaged error in the predicted results by the combustion model (or other CA50 models) [5, 8]. This amount of error fails most advanced control strategies while their nominal benefit

Fig. 1 If using IGA projection, the performance of CA50 prediction degrades in large IGA retard region



is commonly less than 8 %. As a result, there exists strong urge to improve the precision of online CA50 prediction.

Several efforts have been made to improve the CA50 prediction online. One is to carefully parameterize the coefficients of the combustion model according to different running conditions [5, 10]. Similar with the data-fitted torque model, this method can only be accurate on the test-bench and its performance will gradually degrade during long-time running. Another method is to incorporate with a polynomial-fitted map that projects CA50 using ignition timing and combustion duration [8]. Figure 1 summarizes the performance of polynomial-fitted method through a plot of the IGA shift with respect to CA50 shift. It illustrates a fact that there exists more than 20 % fitting error in large ignition retard region. Such amount of error jeopardizes an optimization scheme using CA50 values.

This paper will propose a new method to improve the accuracy of CA50 prediction in large retard region which can be implemented in real-time operation. The new method employs a normalized IMEPH-CA50 characteristic curve to modulate the raw predictions of the combustion model. The engine IMEPH-CA50 characteristic curve has been found through experimental measurements on the test-bench and proven to be representative for wide engine selections and conditions [10]. In Sect. 2.2, experiments will show that the predicted IMEPH-CA50 results, which are calculated by the combustion model, also converge towards the characteristic curve with slightly larger excursion than the measured data do. Section 2.3 will reveal the analytical principle of the IMEPH-CA50 characteristic curve by investigating into the physics of a combustion cycle. Then this knowledge is used to formulate a “validity region” of IMEPH-CA50 prediction. Section 2.4 will integrate all model segments and propose a method to use the “validity region” as a criterion to distinguish and modulate the raw predictions. Section 3 will show the approach of the validation and the actual performance of our overall method.

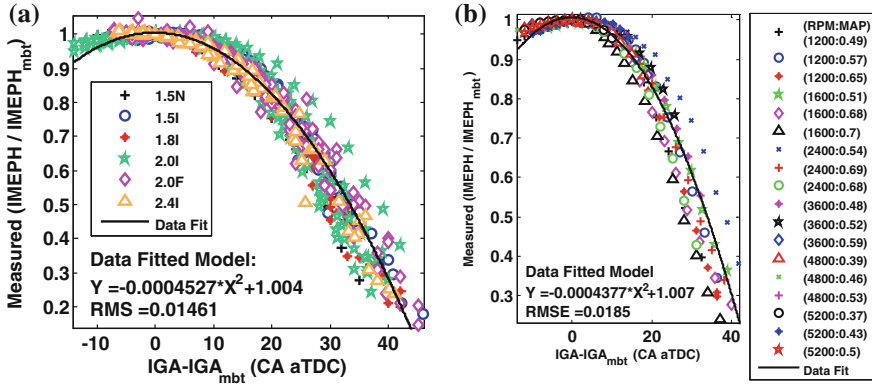


Fig. 2 The nomarlized IMEPH with respect to the ignition retarded from MBT showing the performance of the data-fitted torque model for **a** six different engines; **b** 2.0I engine of different engine speeds (RPM) and manifold-air-pressure (MAP) loads in (bar), with parabolic curve found by data-fitting technique

2 The Online Torque and Combustion Model

2.1 The Data-Fitted Torque Model: The Conventional Way

In the case of ignition retard from MBT timing, conventional ECUs of a light duty vehicle estimate gasoline engine torque, or $IMEPH$, using a MBT value and a scale function, as shown below in Eq. (1).

$$\widehat{IMEPH} = IMEPH_{MBT}(m_{air}, N)h(\Delta\theta) \quad (1)$$

where $IMEPH_{MBT}$ is the nominal MBT torque value which is almost proportional to the inducted air mass m_{air} and engine speed $N \cdot h(\Delta\theta)$, which is a scalar between 0 and 1, is the normalized torque loss due to ignition timing retarded from MBT, or $\Delta\theta$. A small amount of experiments have discovered that $h(\Delta\theta)$ is quite monotonic with little dependency on other engine variables [11]. ECU makers concluded such property and formulated a 1-D map between $\Delta\theta$ and h . Then the tabulated map is used in either torque estimation, or air mass calculation from a torque request. When applying this method to engine fleets, engineers employ slight calibration on h values. The performance of such practice is investigated in Fig. 2a. Although the data-fitted curve, which represents h , can cover the majority of data points, it still cannot explain wild data excursion (more than 18 % fitting error) in large IGA retard region. Figure 2b shows a single-engine data series for 2.0I engine and reveals that data series are isolated for different engine speeds and loads. The 18 % fitting error challenges the presumption that h is univariate. It urges a replacement of a new torque model which can bring more accuracy in large ignition retard region.

2.2 The Combustion Model: Predicting Engine Torque From Combustion

In addition to the low accuracy, there is another motivation to replace the data-fitted torque model: the current model is ignorant of detail combustion dynamics and thus vulnerable during aging. This phenomenon actually exemplifies a dilemma in engine modeling: the more a model relies on calibration (or the less on physical modeling), the less robustness it has when engine states change. One end of the dilemma is a full-calibration model, as illustrated by the data-fitted model in Eq. (1). The other end of the dilemma is exemplified by a multidimensional computational fluid dynamics (CFD) model which reproduces fluid molecular motions and pressure thermodynamics completely [12]. The CFD model calculates IMEPH via definition Eq. (2) using the predicted in-cylinder pressure P . The CFD model, which is physics-based and therefore employs almost no calibration, turns out to be more robust in life-time torque prediction. However, it is computational expensive and obviously infeasible online.

$$IMEPH = \frac{\int PdV}{V_d} \quad (2)$$

To introduce more physical content in a torque model while still balancing its efficiency, the authors have proposed an online mean-value thermodynamic combustion model [5, 6]. The online combustion model takes in the measurement of cycle initial states and uses a mean-value thermodynamic equation to predict the spatially-averaged fluid states thereafter. On the platform that supports the data-fitted model, the new model only requires a few more slow sensors and thus has remarkable cost-effectiveness on light-duty vehicles. The following equation describes the governing thermodynamics of this method.

$$m_c c_v dT(k) + P(k) dV(k) = dQ_g(k) - dQ_{crbl}(P(k)) - dQ_{ht}(T(k), P(k)) \quad (3)$$

Equation (3) follows the first law of thermodynamics. It treats the chamber as a variant control volume with chemical heat generation dQ_g , mass exchange into the crevice volume dQ_{crbl} , and heat transfer to the ambient dQ_{ht} . The net heat gain by the fluid then is calculated and interpreted in the form of fluid states change, as shown by the left hand side of the equation. In order to calculate the fluid state dynamics, all three terms on the right-hand side need to be modeled. Following the fundamental works by previous researchers, all the energy gain and loss can be calculated using equations in (4). All equations are modified versions of the original ones [9] with improvements in efficiency in large ignition retard region.

$$\begin{aligned} dQ_g(k) &= \eta_c m_f Q_{LHV} dx_b(k) \\ dQ_{ht}(T(k), P(k)) &= h_w(P(k)) A_s(k) (T(k) - T_{wall}) \\ dQ_{crbl}(P(k)) &= \left(h'(k) - u(k) \right) dm_{crbl}(P(k)) \end{aligned} \quad (4)$$

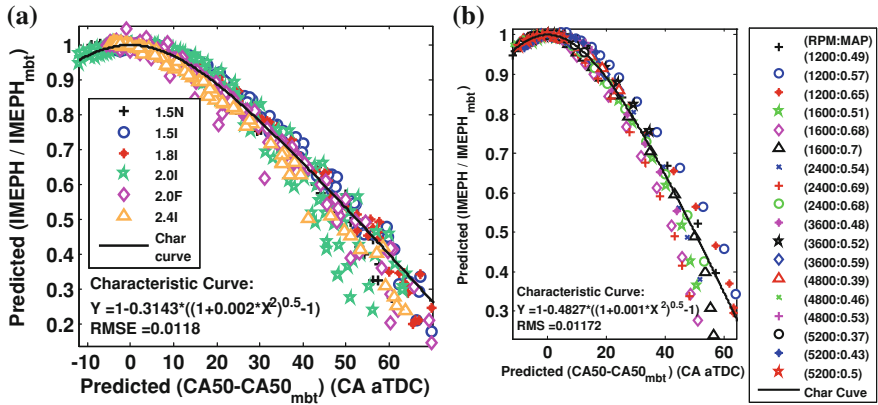


Fig. 3 The strong convergence of the normalized IMEPH-CA50, which are predicted by the online combustion model, towards the engine characteristic curve, found by polynomial-fitting, for **a** different engine selections; **b** single engine plot for 2.0I engine legend in different (RPM:MAP)

The chemical heat release dQ_g is estimated as a “p priori”. The dQ_g is assumed to be proportional to the mass fraction burned dx_b which is predicted from cycle initial states before combustion takes place. The dQ_{ht} is estimated using an enhanced form of the Woschni equation [13]. The dQ_{crbl} is calculated using the mass change inside the crevice dm_{crbl} and their associated enthalpy h' . Note that two terms, dQ_{ht} and dQ_{crbl} , in Eq. (4) are calculated using in-cylinder pressure P and therefore they are “posteriori”. An algorithmic loop exists when solving Eqs. (3) and (4) because the in-cylinder pressure has to be calculated using the knowledge of dQ_{ht} and dQ_{crbl} . In order to solve the loop, a recursive method, as shown in Eq. (5), is applied in implementation so that the calculation of Eq. (3) is proceeded step by step. k is a step counter and the step length can be between 1 CAD and 0.1 CAD depending on user’s decision on resolution.

$$\begin{aligned} T(k+1) &= T(k) + dT(k) \\ P(k+1) &= \frac{m_c R_c T(k+1)}{V(k+1)} \end{aligned} \quad (5)$$

In this way, the entire trajectory of fluid states or P , from intake-valve-closed (IVC) to exhaust-valve-open (EVO), can be calculated. Then IMEPH can be calculated by its definition using Eq. (2). Compared with the data-fitted model, the combustion model reproduces the torque generation process from a combustion process. Figure 3a shows one of the benefit is that the IMEPH results by the combustion model for different engine fleets converge unanimously to the IMEPH-CA50 characteristic curve (found by polynomial-fitting) if it is plotted against CA50 shift. Because of the fact that the engine IMEPH-CA50 characteristic curve can represent a data cluster that are actually measured [11], the convergence of the

predicted results onto the curve implicates its high consistency with the real measurements. This is another strong proof of model's effectiveness.

In Fig. 3a, b, the illustrated IMPEH and CA50 are all predicted results by the combustion model. The CA50 is calculated by the definition $x_b(\theta_{CA50}) = 0.5$, where the mass fraction burned (MFB) profile x_b is an intermediate result of the combustion model. Its calculation follows a modified Weibe function [7], with an additional feature of two stage transition, as shown in Eq. (6):

$$x_b(k) = (1 - \beta_c)x_1(k) + \beta_c x_2(k)$$

$$x_i(\theta(k)) = 1 - \exp \left[-a_{c,i} \left(\frac{\theta(k) - \theta_{soc,i}}{\Delta\theta_i} \right)^{m_{c,i}+1} \right], i = 1, 2 \quad (6)$$

The variable β_c is a transition factor that ranges from 0 to 1 and increases linearly with crank angle. The coefficient $a_{c,i}$ dictates the steepness of the “S” shape of a MFB profile and is subject to change for combustion factors, such as AFR, RGF and IGA. The variable $\Delta\theta_i$ is the combustion duration for each stage and is also a function of the combustion factors. Both $a_{c,i}$ and $\Delta\theta_i$ are found to have highly generic tendency with respect to the combustion factors [5].

Despite of the strong consistency, Fig. 3a also shows that there are some result series deviating from the convergence curve wildly. Figure 3b looks into the specific engine type 2.0I with legends of engine speeds and loads. It clearly shows that the data series for (1600:0.7) and (2400:0.54) speed-load combination have as large as 12 % excursion from the characteristic curve. This amount of error is five times larger than that of the measured IMEPH-CA50. It is determined that the error of convergence in the predicted results is majorly caused by the error in CA50 prediction. It has been discovered that the CA50 prediction by the combustion model has an averaged error of 22 % compared with the measured data [5]. One error source is the stochastic nature of the highly volatile fluid motion in combustion. The other source is the high sensitivity of CA50 on combustion states, as illustrated by the steepness of MFB profile, which further increases the difficulty in prediction. More than 20 % error defies the use of the combustion model in advanced control. Corrections are surely needed to rectify the CA50 prediction towards the actual values.

2.3 The Instant Heat Release Model: The Physical Boundaries of Engine Torque

The question remains how an ECU can know the validity of its prediction during online operation. As mentioned in introduction, online measurements of in-cylinder dynamics can be unacceptably expensive for light-duty vehicles. As a result, a criterion of prediction validity is preferred if it can be calculated analytically from the physics of combustion. Figure 3 implies a candidate criterion for CA50

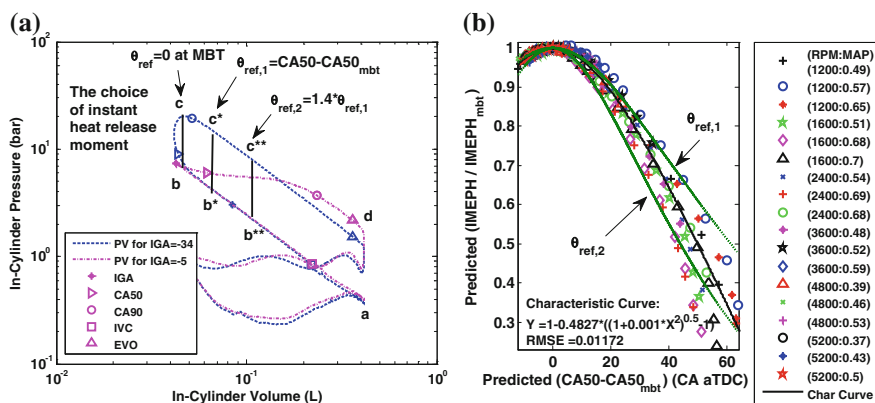


Fig. 4 **a** The schematics of the instant heat release process on the P-V diagram of two typical combustions, one for a MBT ignition timing and the other for a retarded ignition; **b** the two different choices of heat release moment determine the boundaries that enclose IMEPH-CA50 result series, forming a validity region

prediction validity, i.e. the unanimous characteristic curve in the normalized IMEPH-CA50 plot. The scheme then is to use accurate IMEPH prediction to cross-correct the CA50 prediction so that the characteristic curve can be reproduced in the prediction. While strict convergence onto the curve is over-demanding, the authors decided to develop a relaxed version of criterion by computing the up-and-down boundaries which enclose the characteristic curve, forming a “validity region” for prediction. Although manual placement of the boundaries can be performed given sufficient valid data, yet development of the boundary from the combustion physics is preferred for two reasons. First, to understand the physical mechanism behind such boundaries; second, to make sure the boundaries exclude invalid data that are physically impossible. ECUs also want to know an analytic solution of such boundaries in order to calculate them quickly online. To do so, the authors first examine the PV-diagram of a combustion in the case of IGA retard, as shown in Fig. 4a.

Figure 4a illustrates the P-V diagrams of two combustion cycles of different ignition timing. The blue curve for IGA at -34 CA aTDC shows that the areas “a-b-c-d” enclosed by the compression and expansion stroke traces are almost a parallelogram. The IGA therefore maximizes the effective work area “a-b-c-d” and thus maximizes the engine torque given a specific amount of fuel energy. By definition this ignition timing is very close to the MBT timing. On the other hand, the case of IGA at -5 CA aTDC illustrates the negative effect of ignition retard. The retarded IGA ignites the mixture during expansion and raises the fluid pressure in a much slower rate than that in the MBT case. It therefore truncates the effective work area as shown by the enclosed area “a-b-d” in red.

The round curve blue “b-c” or red “b-d” is a thermodynamic process governed by the interaction between combustion heat release, fluid temperature gain and work output to the piston head. The mean-value combustion model, shown

previously in Eqs. (3–6), describes the spatially-averaged fluid behaviour during this period in an efficient way. In order to provide fast estimation of boundaries, further simplifications on the model and the computations are required. One good approximation is to assume that instantaneous heat release (or equivalently, the in-cylinder pressure rise) occurs sharply at the CA of θ_{ref} [8, 10]. Additionally, a polytropic compression and expansion process is assumed because of the high linearity of the log P–V curve in this period. With these two assumptions, the effective work area is then approximated as a parallelogram area “a-b-c-d” in MBT ignition case. By definition shown in Eq. (2), the estimated $IMEPH^*$ can be computed using Eq. (7).

$$IMEPH^* = \left(\frac{P_b V_b^{\gamma_c}}{1 - \gamma_c} \right) \left(V_b^{1-\gamma_c} - V_{BDC}^{1-\gamma_c} \right) - \left(\frac{P_c V_c^{\gamma_e}}{1 - \gamma_e} \right) \left(V_c^{1-\gamma_e} - V_{BDC}^{1-\gamma_e} \right) \quad (7)$$

Polytropic coefficient of expansion and compression are found to be close within an error of 0.01. Thus they are treated as identical, i.e., $\gamma^c = \gamma^e \equiv \gamma$. Since instantaneous heat release is assumed, the cylinder volume before and after heat release is equal at the crank angle θ_{ref} , i.e., $V_b = V_c \triangleq V_{ref} \triangleq V(\theta_{ref})$. And using the equivalent polytropic conversion $PV^\gamma = TV^{\gamma-1}$, Eq. (7) is reformed as a function of combustion heat release $\Delta T \triangleq T_c - T_b$ and cylinder volume at the heat release moment V_{ref} , as shown in Eq. (8):

$$IMEPH^* = \left(\frac{\Delta T}{1 - \gamma} \right) \left(1 - \left(\frac{V_{ref}}{V_{BDC}} \right)^{\gamma-1} \right) \quad (8)$$

In Eq. (8), $IMEPH^*$ reaches maximum as V_{ref} reaches its minimum at V_{TDC} . In MBT case, V_{ref} is close to V_{TDC} as shown by Fig. 4a and thus $V_{ref} = V_{TDC}$ is assigned. In ignition retard case, θ_{ref} will be relocated to θ_{b^*} and the corresponding approximated effective work area will be the parallelogram area enclosed by “a-b*-c*-d”. If a specific amount of fuel is combusted and constant thermal efficiency is assumed, the overall heat release amount ΔT is identical for both ignition cases. Thus the $\overline{IMEPH^*}$, which is the $IMEPH^*$ normalized by $IMEPH_{mbt}$, can be calculated using Eq. (9). Note V_{ref} is the cylinder volume at the moment θ_{ref} , and as a result, $\overline{IMEPH^*}$ is a function of θ_{ref} only.

$$\overline{IMEPH^*}(\theta_{ref}) = \left[1 - \left(\frac{V(\theta_{ref})}{V_{BDC}} \right)^{\gamma-1} \right] / \left[1 - \left(\frac{V_{TDC}}{V_{BDC}} \right)^{\gamma-1} \right] \quad (9)$$

The choice of θ_{ref} is at user’s discretion and is important. It solely determines the how representative the performance boundary is. Geometrically, Fig. 4a shows that at MBT ignition timing, the θ_{ref} can be placed at 0 CAD approximately. For the case of ignition retard, θ_{ref} can be placed at (CA50-CA50_{mbt}) so that the parallelogram area “a-b*-c*-d” can be approximately equal to the area enclosed by the red curve “a-b-d”. Thus the authors choose $\theta_{ref,1} = CA50 - CA50_{mbt}$ and plug into Eq. (9). Figure 4b shows that generally $\overline{IMEPH^*}(\theta_{ref,1})$ overestimates the

torque-loss. The approximate IMEPH is quite accurate in small retard region and yet loses its accuracy gradually as CA50 is further retarded. The reason lies on the fact that in small retard region, the combustion duration is short and the instant-heat-release assumption holds. In the large ignition retarded area, the combustion duration, as exemplified by CA50 in Fig. 1, grows drastically and alters the overall shape of “a-b-c-d”. In this case, the parallelogram area “a-b*-c*-d”, as determined by the assumption, will be larger than the actual area and the difference keeps growing. Figure 4b shows $\overline{IMEPH^*}(\theta_{ref,1})$ sets the up-bound of IMEP-CA50 data series. While the placement of $\theta_{ref,1} = CA50 - CA50_{mbt}$ seems aggressive, a more conservative choice is introduced: $\theta_{ref,2} = 1.4(CA50 - CA50_{mbt})$ as illustrated in Fig. 4a. The model results with $\theta_{ref,2}$ generally under-estimate the torque value as shown in Fig. 4b. It is hypothetical that no combustion has a smaller effective work area than “a-b**-c**-d”. The two curves, $\theta_{ref,1}$ and $\theta_{ref,2}$, encloses the characteristic curve and almost all predicted values of IMEPH-CA50 with a span range of $8 \sim 10\%$.

2.4 “Trinity” Correction Module

The up-bound of the validity region is a value from the ideal combustion case which is impossible to be surpassed. The low-bound is a performance calibre which is not supposed to be breached for a good engine. The “envelope” then becomes a physical principle of reciprocating machines. During online operation, after the $(CA50 - CA50_{mbt})$ is predicted by the online combustion model, the limit of IMEPH will be calculated via Eq. (9). The validity of IMEPH-CA50 prediction can then be checked whether it is within the boundaries. If it is not, ECU will trust IMEPH predictions over CA50 predictions and use the former to cross-correct the latter. The correction criterion is to follow a unanimous characteristic IMEP-CA50 curve. While true values of the characteristic curve is unknown online, the curve can be surrogated by a polynomial curve that is fitted over cascaded raw predictions during online operation, as demonstrated in Fig. 3b. The overall structure, named as “TRINITY” module, is illustrated by a flowchart below in Fig. 5.

3 Experiment Validation

In order to validate our model and method, steady-state test runs on various engine selections were conducted with our model running simultaneously with the measurements. The engines used for these experiments are Geely’s SI VVT port-fuel-injection engines with different compression ratios and different VVT configurations. To further diverse the operation conditions, the engines were tested with

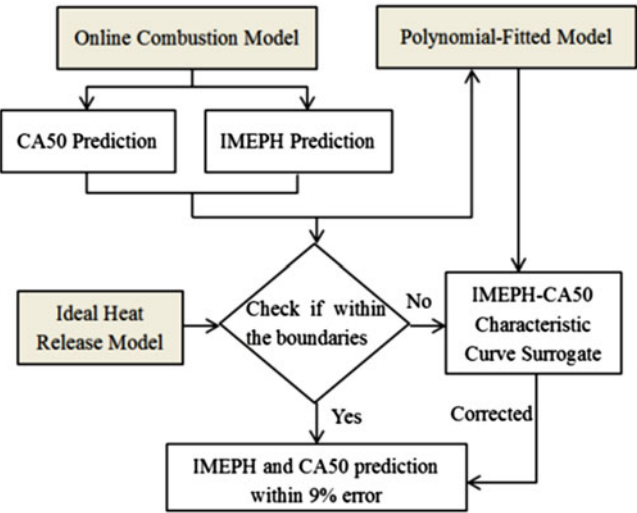


Fig. 5 The “TRINITY” correction module to guarantee the accuracy of CA50 and IMEPH prediction

Table 1 The specifications of experiment engines

Engine number	1.5 N	1.5I	1.8I	2.0I	2.0F	2.4I
Cylinder number	4	4	4	4	4	4
Displacement (L)	1.5	1.5	1.8	2.0	2.0	2.4
Compression ratio	10.3	10.3	10.0	10.0	9.7	10.0
Bore dia. (mm)	77.8	77.8	79.0	85.0	85.0	88.7
Stroke (mm)	78.8	78.8	91.5	88.0	88.0	96.2
Connect rod (mm)	153.3	153.3	129.4	138.6	138.6	130.5
VVT type	Dual ^a	Int ^b	Int	Int	Dual	Int
IVO (CA bTDC)	5.0	5.0	16.0	20.5	20.5	9.8
IVC (CA aBDC)	65.0	65.0	70.5	74.5	74.5	74.2
EVO (CA bBDC)	57.0	57.0	55.5	53.0	53.0	57.8
EVC (CA aTDC)	5.0	5.0	17.0	32.5	30.0	10.2

^a Dual independent VVT. ^b Intake VVT only

different valve lift timings or durations. All engine’s specification are shown in Table 1.

For each test run at an engine speed and load, we first located the MBT point by sweeping the ignition timing. Then we shifted ignition timing from MBT at the step of 2 CAD and conducted steady-state measurements and model calculation for each step. The typical speed selections were 1200, 2000, 2800, 3600, 4000, 4800 and 5200 RPM. The typical load selections were 0.5, 0.6 and 0.7 bar of MAP for each engine speed. All tests were performed with AFR at stoichiometry. All the sensors locations, resolutions, measurements were following the previous experiment setup

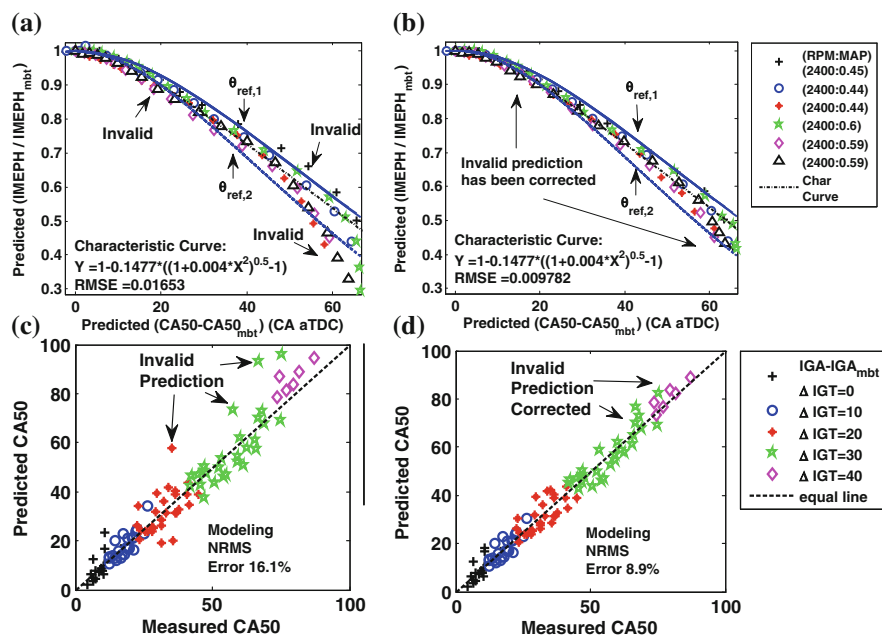


Fig. 6 The “TRINITY” module improved CA50 prediction from 16.1 to 8.9 % when ignition is retarded from MBT timing: **a** and **c** the module first identifies the invalid CA50 prediction on the original prediction; **b** and **d** the invalid IMEPH-CA50 results have been corrected and converged towards the engine characteristic curve and the predicted CA50 has converged towards the actual values

described in [5]. For reference, the test bench measured in-cylinder pressure using a piezoelectric transducer and convert to CA50 and IMEPH readings. To validate our model results, we coded our model in dSPACE rapid hardware prototype and ran the algorithm in real-time. Three torque models were computed parallel and their results are captured and coordinated by the TRINITY module. To compare with the time-averaged measurements, all predictions were averaged using a time frame of 15.6 ms.

First we plotted the normalized IMEPH-IGA data on a single graph for all engines, as shown in Fig. 2a. We then parabola-fitted all data points and reveals 0.01462 RMSE of the data-fitting. We also retrieved the results predicted by the online combustion model and plotted them on a normalized IMEPH-CA50 figure, as shown in Fig. 3a. Compared with Figs. 2a, 3a shows more convergence of data points with 0.0118 RMSE, 20 % less than that of Fig. 2a. Noted in IMEPH-CA50 plot, the CA50 is predicted by our online combustion model and is error-prone. The “TRINITY” correction module is applied on all engines in real time. Figure 6 below show the mechanism of the correction on CA50 predictions as exemplified on 1.5 N engine.

Figure 6a shows that the original IMEPH-CA50 prediction curve has excursions from validity region and they are successfully recognized as “invalid”. Figure 6b shows that after being corrected by “TRINITY” module, the invalid IMEPH-CA50 result points have been shifted inside of the validity region. Correspondently, the corrected CA50 prediction are much more consistent with the actually measured values and the prediction error drops from 16.1 to 8.9 %, as shown by Fig. 6c, d. The benefit of accuracy improvement mainly comes from the convergence of the wide excursions in large ignition retard region. These excursions are the data points with large cycle-to-cycle variation and were previously difficult to predict using the online combustion model.

4 Conclusions

This paper has shown that with the fusion of three torque models, a “hybrid” method to promote the accuracy of IMEPH and CA50 prediction can be developed. The current data-fitted torque model has the simplest IMEPH prediction procedure and therefore suffers accuracy loss in large ignition retard region. The online combustion model renovates the accuracy in that particular region despite of the excursions from the engine characteristic IMEPH-CA50 curve. The inconsistency between the predicted results and the characteristic curve is attributed to error-prone CA50 prediction. In this paper, the authors successfully reconcile the inconsistency by modulating the invalid CA50 predictions according to a surrogate of the characteristic curve. The online identification of the invalid prediction has been proven effective if using a criterion developed based on an ideal-heat-release model. The criterion sets up-and-down torque boundaries of a combustion process and therefore reveals the physical principle of the characteristic curve. Large-scale experiments have validated the effect of our method in CA50 prediction improvement. Further research should employ delicate cycle-to-cycle analysis and reveal the statistical performance of the proposed method.

References

1. Huber W, Lieberoth-Leden B, Maisch W, Reppich A (1991) Electronic throttle control. *Automot Eng Int*, 99(6):15–18
2. Jankovic M, Frischmuth F, Stefanopoulou AG, Cook JA (1998) Torque management of engines with variable cam timing. *IEEE Control Syst Mag* 18(5):34–42
3. Stefanopoulou AG, Cook JA, Freudenberg JS, Grizzle JW (1998) Control-oriented model of a dual equal variable cam timing spark ignition engine. *ASME J Dyn Syst Meas Contr* 120:257–266
4. Hallgren B, Heywood J (2003) Effects of substantial spark retard on SI engine combustion and hydrocarbon emissions, SAE Technical Paper 2003-01-3237. doi:[10.4271/2003-01-3237](https://doi.org/10.4271/2003-01-3237)

5. Qu Z, Ma M, Zhao F (2012) An online crank-angle-resolved mean-value combustion model of gasoline engines including effects of cycle initial states, SAE Technical Paper 2012-01-0129. doi:[10.4271/2012-01-0129](https://doi.org/10.4271/2012-01-0129)
6. Qu Z, Ma M, Zhao F (2012) Estimation and analysis of crank-angle-resolved gas exchange process of spark-ignition engines, SAE Technical Paper 2012-01-0835. doi:[10.4271/2012-01-0835](https://doi.org/10.4271/2012-01-0835)
7. Rausen DJ, Stefanopoulou AG, Kang J-M, Eng JA, Kuo T-W (2005) A mean-value model for control of homogeneous charge compression ignition (HCCI) engines. *J Dyn Syst Meas Control Trans ASME* 127(3):355–362
8. Lee D, Jiang Li, Yilmaz H, Stefanopoulou AG (2010) Preliminary results on optimal variable valve timing and spark timing control via extremum seeking. In: 5th IFAC symposium on mechatronic systems
9. Heywood JB (1988) *Internal combustion engine fundamentals*. McGraw Hill, New York
10. Jiang L, Vanier J, Yilmaz H, Stefanopoulou AG (2009) Parameterization and simulation for a turbocharged spark ignition direct injection engine with variable valve timing. SAE Paper 2009-01-0680
11. Ayala FA, Gerty MD, Heywood JB (2006) Effects of combustion phasing, relative air-fuel ratio, compression ratio, and load on SI engine efficiency, SAE paper 2006-01-0229, Transactions, 115, J Engines, Section 3
12. Kong SC, Marriott CD, Reitz RD (2001) Modeling and experiments of HCCI engine combustion using detailed chemical kinetics with multidimensional CFD, SAE Technical Paper 2001-01-1026. doi:[10.4271/2001-01-1026](https://doi.org/10.4271/2001-01-1026)
13. Woschni G (1967) Universally applicable equation for the instantaneous heat transfer coefficient in the internal combustion engine, SAE Technical Paper 670931. doi:[10.4271/670931](https://doi.org/10.4271/670931)

Proceedings of the FISITA 2012 World Automotive
Congress

Volume 2: Advanced Internal Combustion Engines (II)
; (Eds.)

2013, XIX, 564 p., Hardcover

ISBN: 978-3-642-33749-9